Journal of Alloys and Compounds 506 (2010) 883–887

Contents lists available at ScienceDirect

Journal of Alloys and Compounds

journal homepage: www.elsevier.com/locate/jallcom

Synthesis and electrochemical properties of Li-rich spinel type $LiMn_2O_4$ powders by spray pyrolysis using aqueous solution of manganese carbonate

Shoji Hirose, Takayuki Kodera, Takashi Ogihara*

Department of Material Science and Engineering, University of Fukui, 3-9-1 Bunkyo, Fukui-shi, Fukui 910-8507, Japan

ARTICLE INFO

Article history:
Received 11 February 2010
Received in revised form 13 July 2010
Accepted 13 July 2010
Available online 21 July 2010

Keywords:
Spray pyrolysis
Lithium ion battery
Powders
Rechargeable properties
Surfactant

ABSTRACT

Li-rich lithium manganese oxide ($Li_{1.09}Mn_{1.91}O_4$) powders were prepared by spray pyrolysis using an aqueous solution of manganese carbonate. The aqueous solution, in which manganese carbonate was uniformly dispersed by a surfactant, was used as the starting solution. As observed by scanning electron microscopy, $Li_{1.09}Mn_{1.91}O_4$ had spherical morphology with a porous microstructure and consisted of primary particles. Powder X-ray diffraction analysis revealed that the crystal phase of the $Li_{1.09}Mn_{1.91}O_4$ powders was in good agreement with the spinel phase. Inductively coupled plasma analysis showed that the molar ratio of Li and Mn in the $Li_{1.09}Mn_{1.91}O_4$ powders was 1.09:1.90. Through electrochemical measurements, the initial discharge capacity of a $Li_{1.09}Mn_{1.91}O_4$ cathode was found to be 107 mAh/g at 1 C (99% retention after 100 cycles) and 91 mAh/g at 10 C (93% retention after 100 cycles). The retention ratio of discharge capacity remained greater than 90%, although capacity loss was observed up to 20 cycles. The $Li_{1.09}Mn_{1.91}O_4$ cathode derived from carbonate solution had excellent cycling stability in comparison with the $LiMn_2O_4$ cathode derived from nitrate solution.

1. Introduction

Recently, lithium ion batteries have been expected to become the means of energy storage [1] for electric vehicles (EVs), hybrid electric vehicles (HEVs) and electric tools, as well as for load leveling in photovoltaic power generation. The lithium ion batteries used in these applications require cathode materials that combine low cost, high safety and excellent cycling stability during high-rate charging and discharging. Spinel type $LiMn_2O_4$ cathode materials [2] are thought to be promising for lithium ion batteries in EVs and HEVs, owing to advantages such as low cost, abundant source materials, non-toxicity and high thermal stability. To date, various techniques for preparing $LiMn_2O_4$ cathode materials via liquid-phase reactions [3–10] or solid-state reactions [11–13] have been developed in order to improve the electrochemical properties of the materials, including the cycling stability, rechargeable capacity and recharging rate. We have focused on spray pyrolysis among the liquid-phase reactions. Spray pyrolysis allows for control of particle size, particle size distribution and particle morphology [14]. In addition, the production time required for spray pyrolysis is shorter than that for other liquid-phase reactions. Spray pyrolysis [15–17] has been reported to be a versatile process for synthesizing homogeneous $LiMn_2O_4$, $LiNi_{0.5}Mn_{1.5}O_4$ and $Li(Ni_{1/3}Mn_{1/3}Co_{1/3})O_2$ powders. However, toxic and corrosive gases such as NO_X, Cl_X and SO_X are often discharged during particle formation because reagents such as metal nitrates, chlorides and sulfides are contained in the aqueous starting solution. On the other hand, metal carbonates have not been used as starting materials for spray pyrolysis because of their insolubility in water. If these materials can be used as starting materials, the preparation of the cathode powders will impose a lower environmental load. The preparation of $LiMn_2O_4$ cathode materials by emulsion and solid-state reactions using manganese carbonate has also been reported [18,19]. In the present work, a starting solution for spray pyrolysis was successfully prepared by dispersing manganese carbonate in aqueous solution with a surfactant.

Here, we report the production of $Li_{1.09}Mn_{1.91}O_4$ powders by spray pyrolysis using an aqueous dispersion of manganese carbonate as the starting solution. We also present the particle characterization for these powders. The electrochemical properties of a $Li_{1.09}Mn_{1.91}O_4$ cathode, namely, the rechargeable capacity and cycling performance, were also evaluated. It was well known that $LiMn_2O_4$ exhibits poor cycling stability [20–22] as a result of the Jahn–Teller effect in the recharging process and the dissolution of Mn ions at elevated temperatures. These problems have been addressed by substituting various metal ions [23] at the 16 d sites of the octahedron in the cubic spinel structure. On the other hand, the poor cycling stability of $LiMn_2O_4$ cathodes can also be improved by changing the molar ratio of Li ions and Mn ions. It has been reported that non-stoichiometric $Li_{1+X}Mn_{2-X}O_4$ has excellent

* Corresponding author. Tel.: +81 776 27 8624; fax: +81 776 27 8624.
E-mail address: ogihara@matse.u-fukui.ac.jp (T. Ogihara).

0925-8388/$ – see front matter © 2010 Elsevier B.V. All rights reserved.
doi:10.1016/j.jallcom.2010.07.104

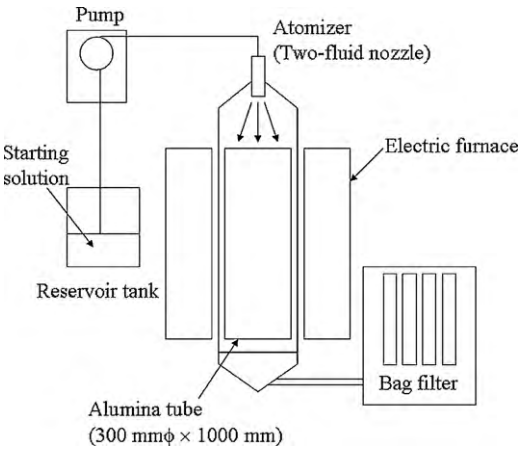

Fig. 1. Spray pyrolysis apparatus used in this work.

cycling stability compared with $LiMn_2O_4$ [24–26]. In the present study, the rechargeable capacity and the cycling performance of a $Li_{1.09}Mn_{1.91}O_4$ cathode prepared by spray pyrolysis were evaluated.

2. Experimental

2.1. Powder preparation

Lithium hydroxide (LiOH, reagent grade, Nacalai Tesque Co. Ltd., Japan) and manganese carbonate ($MnCO_3$, reagent grade, Nacalai Tesque Co. Ltd., Japan) were used as starting materials. $MnCO_3$ consisted of colloidal particles with diameter less than 100 nm and irregular morphology. These were successfully dispersed in aqueous solution by using a surfactant at room temperature. The molar ratio of Li and Mn was set to 1.09:1.91 in the 0.25 mol/dm^3 starting solution, and xanthan gum (0.25 wt%; Roadpole, Rhodia Nicca Co. Ltd., Japan) was added as the surfactant. The pH of the starting solution was adjusted from 4 to 12 using HCl and NH_3OH, which were added in sufficiently small quantities such that corrosion of the electric furnace was avoided and the electrochemical properties of $Li_{1.09}Mn_{1.91}O_4$ were not affected. Xanthan gum is the polysaccharide that consists of glucuronic acid, glucose and mannose. This leads to excellent dispersion stability for $MnCO_3$ in the aqueous solution, because the polysaccharide forms a weak three-dimensional network structure similar to a gel structure.

A large spray pyrolysis apparatus (RH-2, Ohkawara Kakohki Co. Ltd., Japan) was used (Fig. 1), which consisted of a two-fluid nozzle, a cylindrical electric furnace with alumina tube (300 mm⌀ × 1000 mm) as the pyrolysis zone and a bag filter. The starting solution was atomized with the two-fluid nozzle (nozzle diameter: 10 μm). The atomized mist was introduced to the electric furnace by an air carrier gas and then pyrolyzed at 600–800 °C. The flow rate of the carrier gas was 20 dm^3/min, and thus the residence time was about 60 s. $Li_{1.09}Mn_{1.91}O_4$ powders were continuously collected with the bag filters. The powder was then calcined at 800 °C for 4 h in a batch type electric furnace under an air atmosphere.

2.2. Particle characterization of $Li_{1.09}Mn_{1.91}O_4$ powders

The particle morphology and microstructure of the $Li_{1.09}Mn_{1.91}O_4$ powders were determined by scanning electron microscopy (SEM, JSM-6390, JEOL Co. Ltd., Japan). The average particle size was measured by randomly sampling 200 particles from SEM images. The thermal behavior of the as-prepared powders was observed by thermogravimetric-differential thermal analysis (TG-DTA, DTG-60, Shimadzu Co. Ltd., Japan). The crystal phase of the $Li_{1.09}Mn_{1.91}O_4$ powders was identified by powder X-ray diffraction using Cu Kα radiation (XRD, XRD-6100, Shimadzu Co. Ltd., Japan). The specific surface area and average pore size of the $Li_{1.09}Mn_{1.91}O_4$ powders were determined by the BET method (BELSORP-mini, Bel Japan Co. Ltd., Japan). The mesopore distribution of calcined $Li_{1.09}Mn_{1.91}O_4$ powders was determined by the BJH method (BELSORP-mini, Bel Japan Co. Ltd., Japan). The chemical composition of the powders was measured on an inductively coupled plasma analyzer (ICP, SII, SPS-3000 Co. Ltd., Japan).

2.3. Electrochemical properties of $Li_{1.09}Mn_{1.91}O_4$ cathode

The cathode was prepared using 80 wt% $Li_{1.09}Mn_{1.91}O_4$ powder, 10 wt% acetylene black and 10 wt% fluorine resin. Lithium metal (Honjo Chemical) was used as the anode, and a polypropylene sheet (Celgard 2400 Heist) was used as a separator. As an electrolyte, 1 mol/dm^3 $LiPF_6$ (Tomiyama Chemical) in ethylene carbonate/1,2-dimethoxyethane (EC:DEC = 1:1) was used. A 2032 type coin cell was fabricated in a glove box filled with argon. The rechargeable capacity of the $Li_{1.09}Mn_{1.91}O_4$ cathode was measured with a battery tester (BTS2004, Hosen) at between 3.5 V and 4.3 V. The current density ranged from 0.3 mA/cm^2 at 1 C to 6 mA/cm^2 at 10 C.

Table 1
Effect of pH on the dispersion stability of starting solution.

Solution	pH			
	5	6–7	8–10	11
Stability	Precipitation	Unstable	Stable	Stable

3. Results and discussion

3.1. Particle characterization of $Li_{1.09}Mn_{1.91}O_4$ powders

$MnCO_3$ powders were unstable in the aqueous solution without the surfactant, precipitating after a few seconds. $MnCO_3$ could be dispersed in the aqueous solution by using a surfactant and adjusting pH. Table 1 shows the effects of pH on the dispersion stability of $MnCO_3$ powders in the aqueous solution. The dispersion stability was judged from the time required for the $MnCO_3$ powders dispersed in aqueous solution to settle in the test tube. Precipitation occurred after a few minutes when the pH of the aqueous solution was less than pH 4. When the pH of the aqueous solution was greater than pH 5, the dispersion stability of $MnCO_3$ powders was maintained for 30 min in the aqueous solution. The dispersion stability of the solution was maintained for 1 h at greater than pH 8. In particular, when the starting solution with pH 8 was used, $Li_{1.09}Mn_{1.91}O_4$ powders could be successfully prepared. Because the content of NH_3OH used for pH adjustment was less than 1 wt%, this condition was most suitable for the preparation of $Li_{1.09}Mn_{1.91}O_4$ powders with a low environmental load.

Fig. 2(a) shows SEM photographs of as-prepared $Li_{1.09}Mn_{1.91}O_4$ powders obtained when 100 g/h of $Li_{1.09}Mn_{1.91}O_4$ powders was produced. The yield of $Li_{1.09}Mn_{1.91}O_4$ powders was greater than 70% at a production rate of 100 g/h. The particles had a spherical morphology with a porous microstructure. They also had a broad size distribution because the mist atomized by the two-fluid nozzle had a broad size distribution. Fig. 2(b) shows SEM images of $Li_{1.09}Mn_{1.91}O_4$ powders calcined at 800 °C. After calcination, the particles still had a spherical morphology with porous microstructure. Fig. 3 shows the particle microstructure of the as-prepared $Li_{1.09}Mn_{1.91}O_4$ powders and the $Li_{1.09}Mn_{1.91}O_4$ powders calcined at 800 °C. As shown in the SEM image, the $Li_{1.09}Mn_{1.91}O_4$ powders consisted of primary particles of less than 100 nm in diameter. These primary particles were sintered to form $Li_{1.09}Mn_{1.91}O_4$ polycrystals. Fig. 4 shows the BJH plot of $Li_{1.09}Mn_{1.91}O_4$ powders calcined at 800 °C. The pore size distribution of the $Li_{1.09}Mn_{1.91}O_4$ powders broadened, with an average pore size of 12 nm. The specific surface area of $Li_{1.09}Mn_{1.91}O_4$ powders calcined at 800 °C, as determined by the BET method, was about 3 m^2/g.

Fig. 5 shows the crystal phase of the as-prepared $Li_{1.09}Mn_{1.91}O_4$ powders and the $Li_{1.09}Mn_{1.91}O_4$ powders calcined at 800 °C. The crystal phase of the as-prepared $Li_{1.09}Mn_{1.91}O_4$ powders was a spinel structure (Fd3m) with low crystallinity. Other phases such as Li_2CO_3 and Mn_2O_3 were not observed in the as-prepared powders. On the other hand, $Li_{1.09}Mn_{1.91}O_4$ powders with high crystallinity were obtained by the calcination. The a_0 lattice parameter of the calcined $Li_{1.09}Mn_{1.91}O_4$ was 0.8224 nm. It was found that a_0 was smaller than that of $LiMn_2O_4$ (0.8247 nm). This suggests that the addition of excess Li ions led to an increase of Mn^{4+} ions and in turn increased cycling stability. ICP analysis showed that the molar ratio of Li and Mn was 1.09:1.90. The measured chemical composition of the $Li_{1.09}Mn_{1.91}O_4$ powders was in good agreement with the composition of the starting solution. Thus, LiOH and $MnCO_3$ are considered to be uniformly blended in the mist. This suggests that

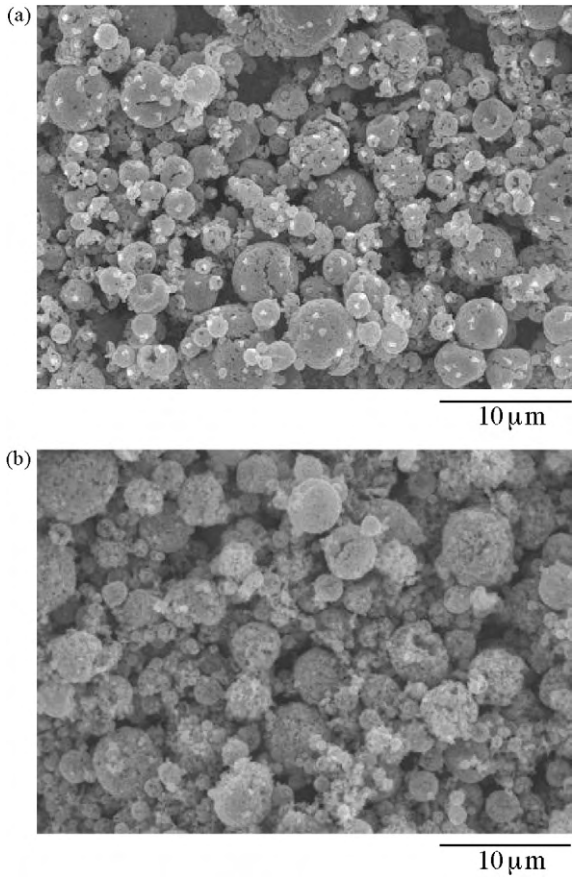

Fig. 2. SEM photographs of $Li_{1.09}Mn_{1.91}O_4$ powders obtained from spray pyrolysis: (a) as-prepared, (b) calcined at 800 °C for 4 h.

the mist play the role of a microreactor and that the solid-state reaction between LiOH and $MnCO_3$ then occurs in the pyrolysis step.

Fig. 6 shows DTA-TG curves of as-prepared $Li_{1.09}Mn_{1.91}O_4$ powders. Weight loss of 2 wt% due to the decomposition of H_2O and CO_2 was observed up to 800 °C in the TG curve. This suggests that H_2O and CO_2 were discharged from the starting solution during pyrolysis and then adsorbed onto the $Li_{1.09}Mn_2O_4$ particles in the bag filter after pyrolysis.

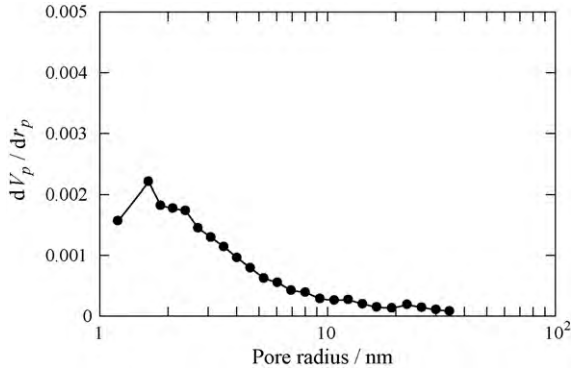

Fig. 4. BJH plot of $Li_{1.09}Mn_{1.91}O_4$ powders calcined at 800 °C for 4 h.

3.2. Electrochemical properties of $Li_{1.09}Mn_{1.91}O_4$ cathode

The rechargeable capacity and cycling stability of a $Li_{1.09}Mn_{1.91}O_4$ cathode were examined by conducting recharging tests. Fig. 7 shows the discharge curves of the $Li_{1.09}Mn_{1.91}O_4$ cathode from 1 C to 10 C. It was found that the voltage jump disappeared in each discharge curve of the $Li_{1.09}Mn_{1.91}O_4$ cathode at 4.1 V, where the discharge curve became a sharp S shape. This suggests that the two phase structure is transformed to a one phase structure in the recharging process [15,27]. The initial discharge capacity of the $Li_{1.09}Mn_{1.91}O_4$ cathode estimated from discharge curve was 107 mAh/g at 1 C. The rechargeable efficiency

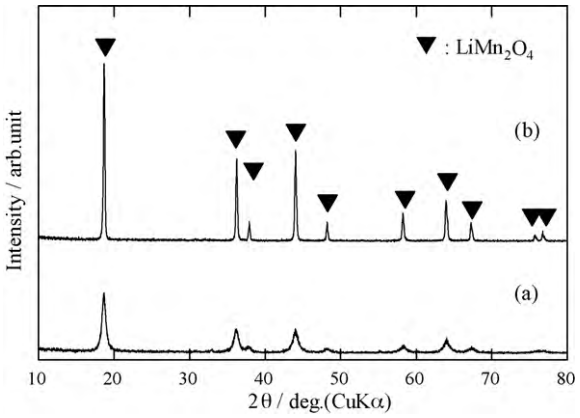

Fig. 5. XRD patterns of $Li_{1.09}Mn_{1.91}O_4$ powders obtained from spray pyrolysis: (a) as-prepared, (b) calcined at 800 °C for 4 h.

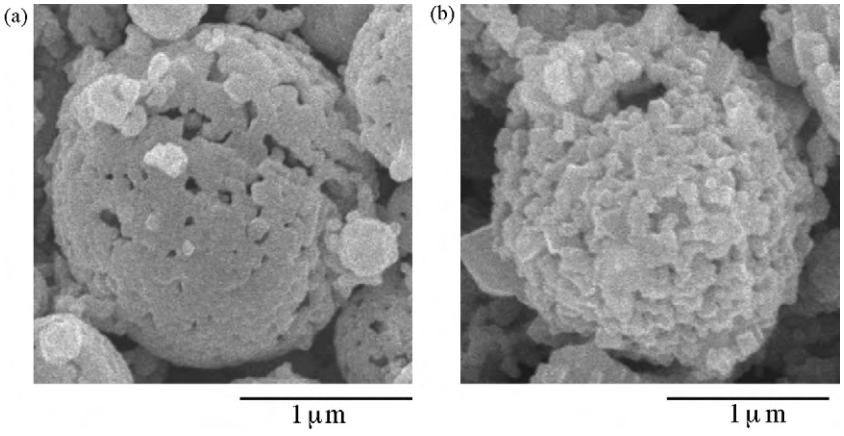

Fig. 3. Particle microstructure of $Li_{1.09}Mn_{1.91}O_4$ powders obtained from spray pyrolysis: (a) as-prepared, (b) calcined at 800 °C for 4 h.

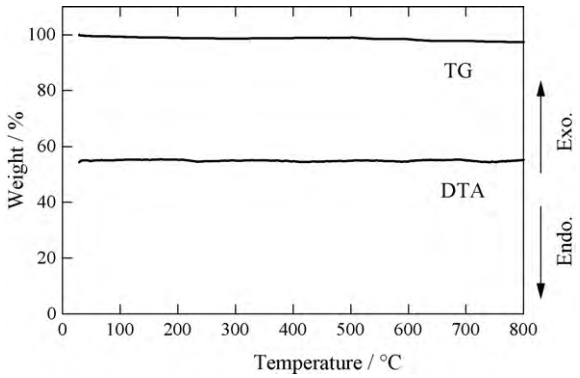

Fig. 6. DTA-TG curves of as-prepared $Li_{1.09}Mn_{1.91}O_4$ powders.

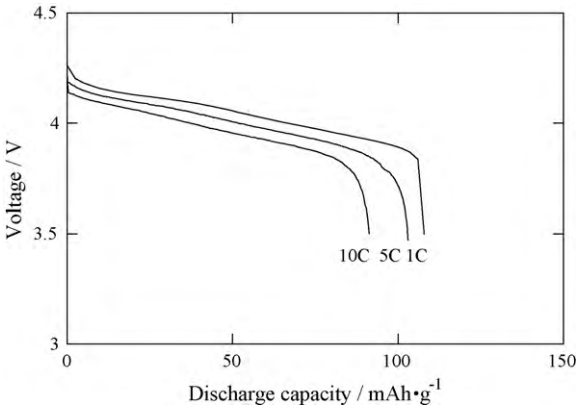

Fig. 7. Discharge curves of $Li_{1.09}Mn_{1.91}O_4$ cathode at rate indicated.

of $Li_{1.09}Mn_{1.91}O_4$ cathode was 97%. The discharge capacity of $Li_{1.09}Mn_{1.91}O_4$ cathode decreased as the discharge rate increased. Specifically, the discharge capacity of the $Li_{1.09}Mn_{1.91}O_4$ cathode decreased to 91 mAh/g at 10 C. The efficiency of discharge capacity was 84% at 10 C. It was found that relatively high discharge capacity was retained at a high discharge rate. From SEM observation, $Li_{1.09}Mn_{1.91}O_4$ powders consisted of primary particles of less than 100 nm in diameter. Smaller primary particles are considered to have shorter diffusion distances for the intercalation of lithium ions, which possibly contributes to the improved discharge rate performance.

Fig. 8 shows the relation between cycle number and discharge capacity of the $Li_{1.09}Mn_{1.91}O_4$ cathode at room temperature. The rechargeable test was carried out up to 100 times from 1 C

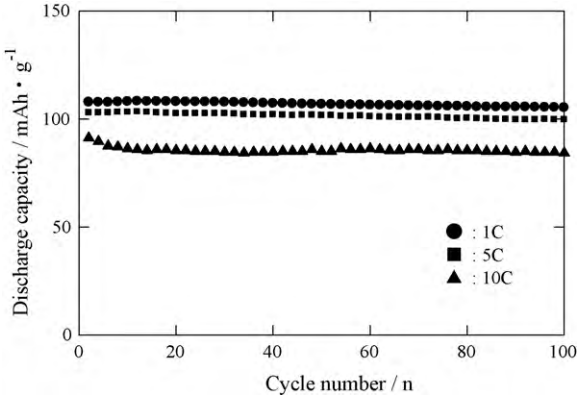

Fig. 8. Relation between cycle number and discharge capacity of $Li_{1.09}Mn_{1.91}O_4$ cathode at rate indicated.

Table 2
Powder characteristics and electrochemical properties of Li-rich $LiMn_2O_4$ and $LiMn_2O_4$ powders obtained from carbonate solution and nitrate solution.

	Carbonate solution	Nitrate solution	
Composition (Li/Mn)	1.09/1.91	1.08/1.2	1/2
Crystal phase	Spinel	Spinel	Spinel
Particle size	1.05	0.84	0.9
Particle size distribution	1.4	1.37	1.3
SSA	3 m^2/g	10 m^2/g	8 m^2/g
Discharge capacity[a]	107 mAh/g	110 mAh/g	115 mAh/g
Cycle stability[b]	99%	95%	90%

[a] 1 C of discharge rate.
[b] Retention ratio of discharge capacity after 100 cycle at 1 C.

to 10 C. The initial discharge capacity of $Li_{1.09}Mn_{1.91}O_4$ cathode was 107 mAh/g at 1 C after 100 cycles. Capacity loss was hardly observed, and the retention ratio of discharge capacity was 99%. The $Li_{1.09}Mn_{1.91}O_4$ cathode exhibited high cycling stability that was the same as that of a metal ion-doped $LiMn_2O_4$ cathode. Moreover, the cycling stability of the $Li_{1.09}Mn_{1.91}O_4$ cathode was superior to that of another Li-rich $LiMn_2O_4$ ($Li_{1.08}Mn_{1.92}O_4$) cathode obtained by spray pyrolysis [28]. The initial discharge capacity of the $Li_{1.09}Mn_{1.91}O_4$ cathode was 85 mAh/g at 10 C after 100 cycles. The retention ratio of the discharge capacity remained greater than 90%, although capacity loss was observed up to 20 cycles. It was found that the porous Li-rich $LiMn_2O_4$ cathode had excellent cycling stability. From these results, we speculate that the porous microstructure may lead to the high cycling stability of the $Li_{1.09}Mn_2O_4$ cathode because the cathode can accommodate the volume change caused by rapid intercalation of lithium ions.

Table 2 shows a comparison of powders characteristics and electrochemical properties of Li-rich $LiMn_2O_4$ cathode materials obtained from carbonate and nitrate solutions. It was clear that the chemical composition of all samples was in agreement with the composition of the starting solution. Li-rich $LiMn_2O_4$ powders derived from carbonate solution had a larger particle size and broader size distribution in comparison with Li-rich $LiMn_2O_4$ powders derived from nitrate solution. The specific surface area of Li-rich $LiMn_2O_4$ powders was significantly smaller than that of Li-rich $LiMn_2O_4$ powders derived from nitrate solution. This possibly resulted in rapid sintering of $MnCO_3$ sols in the mist during pyrolysis. The $LiMn_2O_4$ cathode made from powders derived from nitrate solution had the highest discharge capacity (115 mAh/g), but lower cycling stability than the Li-rich $LiMn_2O_4$ cathode. The Li-rich $LiMn_2O_4$ cathode had excellent cycling stability compared with the $LiMn_2O_4$ cathode. $Li_{1.09}Mn_{1.91}O_4$ cathode derived from carbonate solution had the highest cycling stability (99%) among all samples. It was clear that Li-rich $LiMn_2O_4$ was effective for the improvement of cycling stability.

4. Conclusions

Manganese carbonate could be uniformly dispersed by using a surfactant and adjusting pH. $Li_{1.09}Mn_{1.91}O_4$ powders were successfully prepared by spray pyrolysis using an aqueous solution of manganese carbonate. The particles had spherical morphology with a porous microstructure and consisted of primary particles. The $Li_{1.09}Mn_{1.91}O_4$ powders were well crystallized to a spinel phase by calcination at 800 °C. The chemical composition of $Li_{1.09}Mn_{1.91}O_4$ powders was good agreement with the composition of the starting solution. The discharge capacity of the $Li_{1.09}Mn_{1.91}O_4$ cathode was 107 mAh/g at 1 C, and the rechargeable efficiency was 97%. At 1 C, 99% of the initial discharge capacity was retained after 100 cycles. Moreover, the $Li_{1.09}Mn_{1.91}O_4$ cathode retained 90% of the initial discharge capacity at 10 C. In the future, this process is expected to be an effective means of preparing other metal oxide powders

from the liquid phase in environmentally friendly processes without emission of toxic and corrosive gases such as NO_X, Cl_X and SO_X.

Acknowledgement

This work was supported by the "Development of an Electric Energy Storage System for Grid-connection with New Energy Resources" project of the New Energy and Industrial Technology Development Organization.

References

[1] E. Karden, S. Ploumen, B. Fricke, T. Miller, K. Snyder, J. Power Sources 168 (2007) 2–11.
[2] Z. Pegeng, F. Huiqing, F. Yunfei, L. Zhuo, D. Yongli, Rare Metals 25 (2006) 100–104.
[3] H. Yue, X. Huang, D. Lv, Y. Yang, Electrochim. Acta 54 (2009) 5363–5367.
[4] T.J. Patey, R. Büchel, S.H. Ng, F. Krumeich, S.E. Pratsinis, P. Novák, J. Power Sources 189 (2009) 149–154.
[5] C. Wan, M. Wu, D. Wu, Powder Technol. 199 (2010) 154–158.
[6] K. Ragavendran, D. Sherwood, D. Vasudevan, B. Emmanuel, Phys. B: Condens. Matter 404 (2009) 2166–2171.
[7] X. Liu, Z. Huang, S. Oh, P. Ma, C.H. Chan, G.K. Vedam, K. Kang, J. Kim, J. Power Sources 195 (2010) 4290–4296.
[8] J. Park, S. Kim, J. Park, C. Hwang, M. Choi, J. Kim, K. Ok, H. Kwak, Il. Shim, Mater. Lett. 63 (2009) 2201–2204.
[9] Y. Fu, Y. Su, C. Lin, S. Wu, Ceram. Int. 35 (2009) 3463–3468.
[10] Q. Zhang, S. Li, S. Sun, X. Yin, J. Yu, Chem. Eng. Sci. 65 (2010) 169–173.
[11] N. Kitamura, H. Iwatsuki, Y. Idemoto, J. Power Sources 189 (2009) 114–120.
[12] Q. Liu, L. Yu, H. Wang, J. Alloys Compd. 486 (2009) 886–889.
[13] N. Kamarulzaman, R. Yusoff, N. Kamarudin, N.H. Shaari, N.A. Aziz, M.A. Bustam, N. Blagojevic, M. Elcombe, M. Blackford, M. Avdeev, A.K. Arof, J. Power Sources 188 (2009) 274–280.
[14] G.L. Messing, S.C. Zhang, G.V. Javanthi, J. Am. Ceram. Soc. 76 (1993) 2707–2726.
[15] T. Ogihara, T. Kodera, K. Myoujin, S. Motohira, Mater. Sci. Eng. B 161 (2009) 109–114.
[16] L. Zhang, T. Yabu, I. Taniguchi, Mater. Res. Bull. 44 (2009) 707–713.
[17] S. Ju, Y. Kang, J. Alloys Compd. 469 (2009) 304–309.
[18] K. Du, G. Hu, Z. Peng, L. Qi, Electrochim. Acta 55 (2010) 1733–1739.
[19] H. Guo, X. Li, Z. Wang, W. Peng, X. Cao, H. Li, J. Power Sources 189 (2009) 95–100.
[20] M.M. Thackeray, J. Electrochem. Soc. 142 (1995) 2558–2563.
[21] A. Kock, E. Ferg, R.J. Gummow, J. Power Sources 70 (1998) 247–252.
[22] H. Kobayashia, H. Sakaebe, K. Komoto, H. Kageyama, M. Tabuchi, K. Tatsumia, T. Kohigashi, M. Yonemura, R. Kanno, T. Kamiyama, Solid State Ionics 156 (2003) 309–318.
[23] K.M. Shaju, G.V. Subba Rao, B.V.R. Chowdari, Solid State Ionics 148 (2002) 343–350.
[24] M. Yoshio, Y. Xia, K. Ikeda, H. Noguchi, Mater. Res. Soc. Symp. Proc. 393 (1995) 41–50.
[25] Y. Xia, H. Noguchi, M. Yoshio, J. Solid State Chem. 119 (1995) 216–218.
[26] Z. Peng, Q. Jiang, K. Du, W. Wang, G. Hu, Y. Liu, J. Alloys Compd. 493 (2010) 640–644.
[27] D. Guyomard, J.M. Tarascon, Solid State Ionics 69 (1994) 222–227.
[28] K. Myojin, T. Ogihara, N. Ogata, N. Aoyagi, H. Aikiyo, T. Ookawa, S. Omura, M. Yanagimoto, M. Uede, T. Oohara, Adv. Powder Technol. 15 (2004) 397–403.